PAPER • **OPEN ACCESS**

Mathematical modelling of fluid flow in electromagnetically stirred weld pool

To cite this article: K Enger *et al* 2021 *IOP Conf. Ser.: Mater. Sci. Eng.* **1201** 012025

Mathematical modelling of fluid flow in electromagnetically stirred weld pool

K Enger*, M G Mousavi and A Safari

Dept. of Science and Industry Systems, University of South-Eastern Norway (USN), Kongsberg, Norway

* Contact author: kjell.enger@usn.no

Abstract. In this paper, a mathematical model has been proposed to study the relationship between electromagnetic stirring (EMS) weld parameters and the mode of fluid flow on grain refinement of AA 6060 weldments. For this purpose, fluid flow modelling using Navier-Stokes equation is described first, and then, the proposed mathematical approach has been discussed in detail. For demonstration, calculations to determine the fluid velocity in the weld pool of thin plate AA6060 were performed. The application of the model on the experimental results indicates that the best grain refinement is achieved at a transition mode from laminar to turbulent fluid flow.

1. Introduction

Refinement of the grain structure in aluminium casts and welds is thought to provide improved mechanical qualities and the grain structure of typical gas tungsten arc (GTA) welds is dependent on both welding conditions and alloy content [1-3]. Weld pool stirring can also be used to achieve significant grain refinement in aluminium welds. The solid-liquid mixture can stay a fluid with high solid fractions if the molten metal is stirred, at which point the equiaxed dendrites become coherent with the solid skin [4]. Brown et al. [5] discovered in 1962 that applying an alternating axial magnetic field (parallel to the arc axis) generated a Lorentz force in the weld pool due to interaction between welding current and the imposed magnetic flux. The impact of EMS during TIG welding on grain size, hot cracking, and porosity, as well as fusion line grain separation in certain Aluminium alloys has been studied [6-9]. The thermal conditions in the weld pool, which are in turn dependent on the set welding parameters, determine the solidification morphology and growth pattern. Stirring, primarily, changes the thermal conditions in the weld pool and consequently affects the growth rate and solidification morphology [9].

In this work, the relationship between the EMS weld parameters and the mode of fluid flow in the weld pool has been studied, by proposing a model to understand the relationship between optimized grain refinement and fluid flow rates, in AA 6060 EMS weldments.

2. Approach

2.1. Fluid flow model: The theory

Interaction between the imposed magnetic induction and the welding current introduces the principle of EMS during welding. And based on that, a Lorentz force is created in the weld pool. The welding current is radially spread in the workpiece throughout TIG welding. A Lorentz force (F_L) is obtained since an

external magnetic field is applied axially (i.e., parallel to the arc axis). Its direction follows the Fleming's left-hand rule and is perpendicular to both the current density (J) and magnetic induction (B), hence, it can be represented by:

$$F_L = J \times B \times \sin\alpha \tag{1}$$

where α is the lowest angle between the current density and the magnetic inductance vector.
Principally, as a result of the combination of four various forces, weld pool (unstirred) convection can occur [10], namely, self-induced electromagnetic force, buoyancy force, surface tension, and aerodynamic drag force. The combination of these forces results in a highly complicated convection pattern. There are two useful equations, namely (1) continuity equation and (2) Navier-Stokes moment equation, that are used to simulate the convection in the weld pool. In the case where the density and viscosity of the fluid are constant, these equations can be shown as follows [11,12]:

$$\text{Continuity equation: } \nabla \cdot \mathbf{v} = 0 \tag{2}$$

Navier-Stokes momentum equation:

$$\rho\left(\frac{\partial \mathrm{v}}{\partial \mathrm{t}} + \mathrm{v}.\nabla \mathrm{v}\right) = -\nabla \mathrm{p} + \eta \nabla^2 \mathrm{v} - \rho\beta \mathrm{g}(\mathrm{T} - \mathrm{T}_0) + \mathrm{j} \times \mathrm{B} \tag{3}$$

where v is the fluid velocity, ∇p is the static pressure, $\eta \nabla^2 v$ is the viscous force, $\rho\beta g(T-T_0)$ is the buoyancy force and $j \times B$ is the Lorentz force. Considering cylindrical coordinates and neglecting the buoyancy force, equation (3) can be expressed in its azimuthal (ϕ) component as follows [12]:

$$\rho\left(\frac{\partial \mathrm{v}_\phi}{\partial \mathrm{t}} + \frac{\mathrm{v}_\mathrm{r}}{\mathrm{r}}\frac{\partial \mathrm{r}\mathrm{v}_\phi}{\partial \mathrm{r}} + \mathrm{v}_\mathrm{z}\frac{\partial \mathrm{v}_\phi}{\partial \mathrm{z}} + \frac{\mathrm{v}_\phi}{\mathrm{r}}\frac{\partial \mathrm{v}_\phi}{\partial \phi}\right) = -\frac{1}{\mathrm{r}}\frac{\partial \mathrm{p}}{\partial \phi} + \mathrm{j}_\mathrm{r} \parallel \mathrm{B}_\phi + \eta \nabla^2 \mathrm{v}_\phi \tag{4}$$

The radial and axial components of equation (3) do not include the Lorentz force and are not relevant to our case. From equation (4) it can be seen that the Lorentz force will cause the liquid in the weld pool to rotate azimuthally. This rotation can be done in two directions; clockwise or anti-clockwise, representing unidirectional stirring or it can be the combination of both i.e., alternating stirring. It is believed that the latter is responsible for weld metal grain refinement [6].

2.2. Mathematical approach

During EMS, the liquid metal flow in the weld pool can be analysed by solving equation (4). In the case of unidirectional stirring, de Vries [13] has proposed a simplified solution for this equation. By this solution, the fluid velocity ($v\phi$) at any distance (r) from the weld centreline can be achieved by equation (5):

$$\mathrm{v}_\phi = \frac{\mathrm{B}\mathrm{I}_\mathrm{W}}{16\pi \mathrm{d}\eta}\left(\mathrm{r} - \frac{\mathrm{r}^3}{\mathrm{R}^2}\right) \tag{5}$$

where η is the liquid metal viscosity, I_W is the welding current, R is the radius of the fusion zone, and also the plate thickness is shown by the parameter (d). It is assumed that, during static unidirectional stirring, the velocity of the liquid metal at the center of the pool (r = 0) as well as at the fusion boundary (r = R) is equal to zero. The fluid velocity v_ϕ at any distance from centre ($0 < r < R$) may be described as increasing from 0 at the time (t=0) to a maximum at the time ($t \approx \infty$), if the equation (5) is reliable for a steady-state condition (time $\approx \infty$). Therefore, the fluid flow at transient state will be solved by equation (5) for v_ϕ as a function of time t [18], [23].

Let us assume to have a cylinder weld pool with radius R, height d and a current distribution pattern as schematically illustrated in Figure 1. It is supposed that the current density is constant at the surface of weld pool.

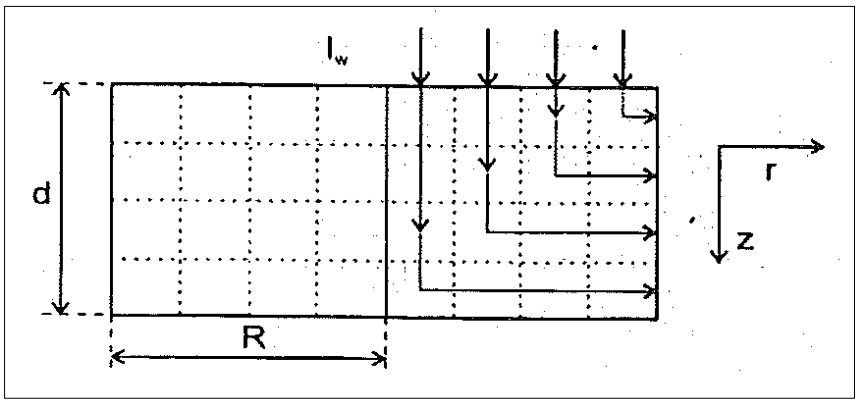

Figure 1. Current distribution in two axial (z) and radial (r) directions of a cylindrical weld pool [13]

For the case of unidirectional stirring, the Lorentz force on a volume element of liquid metal is applied as follows, when the magnetic induction in magnitude and direction is constant[13, 21]:

$$F_L = J_r \times B = \frac{BI_w}{2\pi R^2 d} r \tag{6}$$

Substituting equation 6 into equation (4) results in the following equation:

$$\rho\left(\frac{\partial v_\phi}{\partial t} + \frac{V_r}{r}\frac{\partial r v_\phi}{\partial r} + v_z\frac{\partial v_\phi}{\partial z} + \frac{v_\phi}{r}\frac{\partial v_\phi}{\partial \phi}\right) = -\frac{1}{r}\frac{\partial p}{\partial \phi} + \frac{BI_w}{2\pi R^2 d} r + \eta \nabla^2 v_\phi \tag{7}$$

Assuming the azimuthal component of the fluid flow and the arc pressure are homogeneous ($\partial v_\phi / \partial \phi = 0$ and $\partial p / \partial \phi = 0$), while the radial and the axial components of fluid velocity are neglect, equation (7) can be summarized to:

$$\rho\left(\frac{\partial v_\phi}{\partial t}\right) = \eta \frac{\partial}{\partial r}\frac{1}{r}\frac{\partial (r v_\phi)}{\partial r} + \frac{BI_w}{2\pi R^2 d} r \tag{8}$$

Further, we may assume that the total rotational fluid flow $v_\phi(r,t)$ can be written as the sum of the fluid flow at steady state $s_\phi(r)$ and transient state $u_\phi(r,t)$ i.e.:

$$v_\phi(r,t) = s_\phi(r) + u_\phi(r,t) \tag{9}$$

From the combination of equation (8) and (9):

$$\rho\left(\frac{\partial (s_\phi(r) + u_\phi(r,t))}{\partial t}\right) = \eta \frac{\partial}{\partial r}\frac{1}{r}\frac{\partial (r(s_\phi(r) + u_\phi(r,t)))}{\partial r} + \frac{BI_w}{2\pi R^2 d} r \tag{10}$$

Substitution of equation (5) (replacing v_ϕ by u_ϕ) into equation (10) yields:

$$\rho\left(\frac{\partial u_\varphi(r,t)}{\partial t}\right) = \eta \frac{\partial}{\partial r}\frac{1}{r}\frac{\partial (r(u_\varphi(r,t)))}{\partial r} \tag{11}$$

Employing Separation of Variable Method [$u_\phi(r,t) = X(r)T(t)$] [14] equation (11) can be solved by setting the boundary conditions $X(r) = 0$ at $r = 0$ and $r = R$ as:

$T(t) = C_1 e^{-\lambda^2 t}$ and $X(r) = C_2 J_1(\lambda R\sqrt{\rho/\eta})$, where C_1 and C_2 are constant coefficients, λ is equal to $(3.83/R)(\eta/\rho)^{1/2}$ and $J_1(\lambda R\sqrt{\rho/\eta})$, is the Bessel Function of the first order for $\lambda R\sqrt{\rho/\eta}$. At initial condition ($v_\phi(r,t) = 0$ at $t = 0$), C_1 and C_2 could be determined, which results in:

$$u_\phi(r,t) = \frac{BI_w}{16\pi d\eta}\left(-r + \frac{r^3}{R^2}\right)e^{-\lambda^2 t}$$

and hence,

$$v_\phi(r,t) = \frac{BI_w}{16\pi d\eta}\left(r - \frac{r^3}{R^2}\right)(1 - e^{-\lambda^2 t}) \quad (12)$$

3. Results and discussions

As a demonstrative example, calculations to determine the fluid velocity in the weld pool of thin plate AA6060 were performed, using equation (12). The material properties and EMS welding parameters of this experiment are given elsewhere [6, 13, 15]. The result of the model prediction is presented in Figure 2, which illustrates the variation in fluid flow rate V_ϕ as a function of time t and distance from weld centreline r.

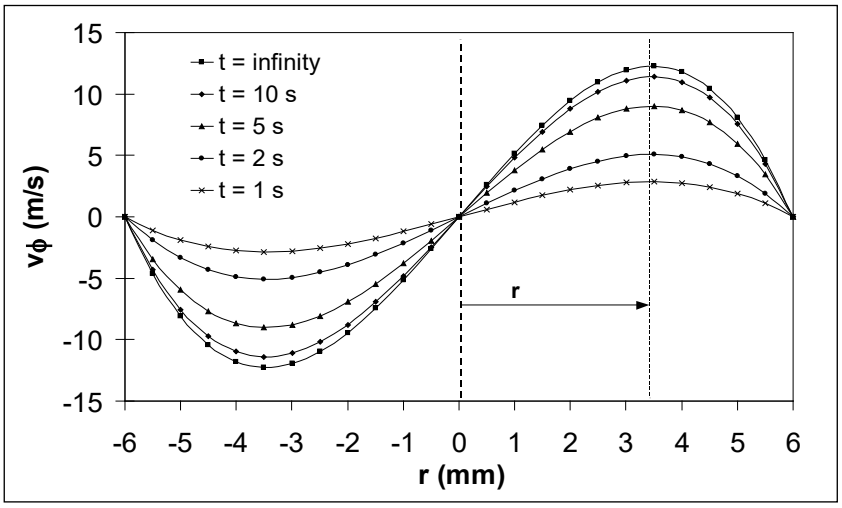

Figure 2. Calculated fluid velocity v_ϕ, in a static weld pool of a thin plate (3 mm) during EMS. The fluid velocity is illustrated as a function of the distance from the weld pool centre at various elapsed times t during unidirectional stirring.

It is assumed that the fluid velocity at a certain r as a function of time has a sinusoidal form, the velocity profile and its relationship with the magnetic field signal can be demonstrated as in Figure 3.

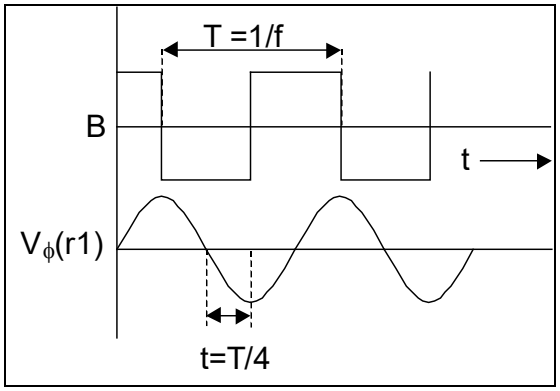

Figure 3. Schematic diagram of the velocity profile and its relationship with the magnetic field signal [15].

In case of alternating stirring, one may consider that the time for each complete rotation is equal to T=1/f and t=1/4T or t=1/(4f), at any magnetic induction intensity, we can calculate the rate of fluid flow at different frequencies (1/T).

From Figure 3, it can be assumed that the essential time for the fluid to achieve the highest velocity from 0 conditions during alternating stirring is equal to a quarter of its one cycle stirring period t = 0.25T or $t = (4f)^{-1}$. Using this assumption, the maximum amount of fluid velocity during alternating stirring can then be estimated through equation (12). Figure 4 illustrates the schematic comparison between the unidirectional and alternatingly stirred fluid flow [19].

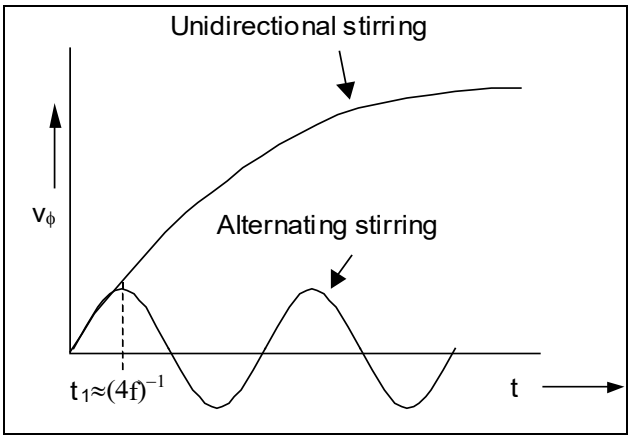

Figure 4. Schematic illustration showing a comparison between a unidirectional stirred fluid flow and an alternatingly stirred fluid flow [15].

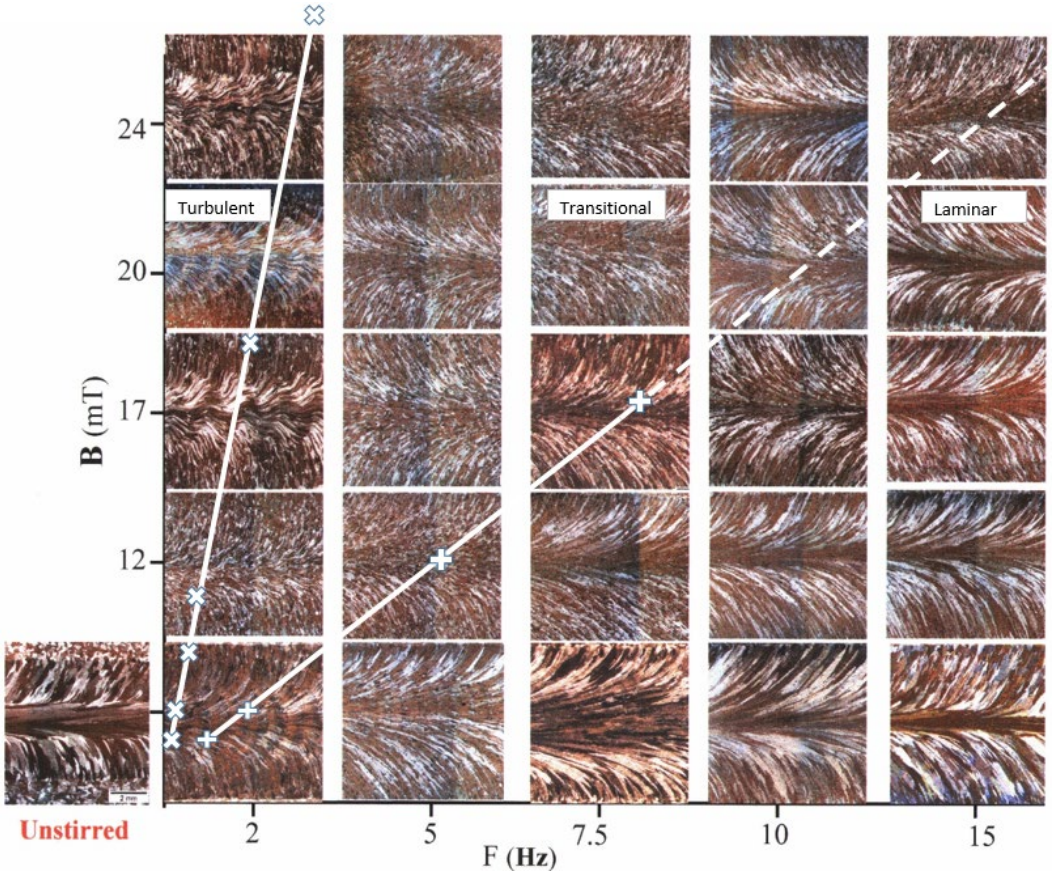

Figure 5. The AA6060-T6 GTA welds from top-view gained without EMS (left) and with EMS. Dotted white lines are modes of fluid flow, according to the Model's prediction in the stirred welds.

According to fluid mechanics and taking an analogue flow pattern i.e., fluid flow in open channels it is possible to determine the mode of flow in the weld pool. On the case of open channels, the Reynolds Number for laminar flow is given as: Re < 500, and for turbulent flow: Re > 2000 [16, 22].

From these values and using the model it is possible to calculate their corresponding velocities in the weld pool during stirring. By extrapolating these velocities (dotted white colour lines) into the result shown in Figure 5 [6], the improved EMS parameters in order to grain refinement could be proposed. By incorporating calculated velocities into micrographs, we can observe that grain refining owing to EMS occurs at a certain stirring frequency and magnetic field strength, which corresponds to the transition condition from laminar to turbulent fluid flow [17, 20].

4. Conclusions

The developed model in this study predicted that the optimum grain refinement due to EMS welding is achieved at a transient fluid flow rate from laminar to turbulent flow. Here, an optimum grain refining, due to EMS, besides stirring frequency and the magnetic field strength is also a function of welding current and weld pool radius.

References

[1] Pearce B P and Kerr H W 1981 Grain refinement in magnetically stirred GTA welds of aluminium alloys, *Metall. Trans. B.***12**, 479–86.
[2] Ganaha T and Kerr H W 1978 TIG weld solidification structures in carbon sheet steels, *Met. Technol.*. **5**, 62-9.
[3] Mousavi M G 1999 PhD thesis *NTNU* Trondheim Norway.
[4] Tzavaras A A and Brody H D 1984 Electromagnetic stirring and continuous casting — Achievements, problems, and goals, *J Miner., Met. Mater Soc.,* **36**, 31-7.
[5] Mousavi M G 2014 Grain refinement and elimination of hot cracks due to application of electromagnetic stirring in commercial aluminium alloy welds, *Adv. Mater. Res.* 1306-11.
[6] Mousavi M G, Yudodibroto B Y, Hermans M J M, and den Ouden G 2001 Effects of electromagnetic stirring during GTA welding on grain structure of AA6060. *Proc. JOM-10 Conf.,* (Helsingor Denmark: 2001)
[7] Mousavi M G, Hermans M J M, and den Ouden G 2001 Effects of electromagnetic stirring on hot cracking susceptibility of aluminium alloy welds. *Proc. JOM-10 Conf.,* (Helsingor Denmark: 2001)
[8] Mousavi M G, Hermans M J M, and den Ouden G 2003 Grain detachment vs. dendrite fragmentation in aluminium stirred welds, *Sci. Technol. Weld. Joining,* **8** (4), 309-12.
[9] Mousavi M G, Hermans M J M, and den Ouden G 2005 Effect of EMS on weld pool porosity in aluminium alloy 7020, *12th Int. Conf. Joining Mater. Proc. JOM-12 conf.* ISBN: 87-89582-13-6, (Helsingor Denmark: 2005)
[10] Matsunawa 1992 Modelling of heat and fluid flow in arc welding, *Int. Trends Weld Sci. Technol. Proc. 3rd Int. Conf. Trends Weld. Res.* (Gatlinburg: 1992)
[11] Fanchi J R 2010 *Integrated Reservoir Asset Management*, ISBN 978-0-12-382088-4.
[12] Rutherford A 1965 Vectors, tensors, and the basic equations of fluid mechanics, *Am. Math. Mon.* **72.** DOI:10.2307/2313035.
[13] Vries H 1998 PhD thesis *Delft University,* The Netherlands.
[14] Boyce W E and DiPrima R C 1997 Elementary differential equation and boundary value problems *John Wiley & sons. Inc.* New York.
[15] Yudodibroto B Y 2000 The effect of electro-magnetic stirring on the weld microstructure of aluminium alloys, Master Thesis *TU Delft,* The Netherlands.
[16] Mott R L 1990 Applied fluid mechanics, *Prentice Hall* NJ Ohio US.
[17] Meng X, Artinov A, Bachmann M, and Rethmeier M 2020 Theoretical study of influence of electromagnetic stirring on transport phenomena in wire feed laser beam welding, *J Laser Appl.* **32** (2). DOI: 10.2351/7.0000069.

[18] Bachmann M, Avilov V, Gumenyuk A, and Rethmeier M 2015 Experimental and numerical investigation of an electromagnetic weld pool support system for high power laser beam welding of austenitic stainless-steel, *J. Mater. Process Technol.* **214**(3) 578-91.
[19] Bachmann M, Kunze R, Avilov V, and Rethmeier M 2016 Finite element modelling of an alternating current electromagnetic weld pool support in full penetration laser beam welding of thick duplex stainless-steel plates, *J. Laser Appl.* **28**, 022404.
[20] Chen J, Wei Y, Zhan X, Gu C, and Zhao X 2018 Thermoelectric currents and thermoelectric-magnetic effects in full-penetration laser beam welding of aluminium alloy with magnetic field support, *Int. J. of Heat Mass Trans.* **127**, 332-44.
[21] Gatzen M, Tang Z, and Vollertsen F 2011 Effect of electromagnetic stirring on the element distribution in laser beam welding of aluminium with filler wire, *Phys. Procedia* **12**, 56-65.
[22] Muhammad S, Han S W, Na S J, Gumenyuk A, and Rethmeier M 2018 Study on the role of recondensation flux in high power laser welding by computational fluid dynamics simulations, *J. Laser Appl.*, **30**, 012013.
[23] Meng X, Bachmann M, Artinov A, and Rethmeier M 2019 Experimental and numerical assessment of weld pool behaviour and final microstructure in wire feed laser beam welding with electromagnetic stirring, *J. Manuf. Processes* **45**, 408–18.